Macromolecules
COMMUNICATION TO THE EDITOR

Macromolecules **2009**, *42*, 3841–3844 **3841**
DOI: 10.1021/ma900796b

Metastable Nematic Preordering in Smectic Liquid Crystalline Phase Transitions

Nasser Mohieddin Abukhdeir* and Alejandro D. Rey

Department of Chemical Engineering, McGill University, Montréal, Québec H3A 2B2, Canada

Received April 11, 2009
Revised Manuscript Received May 4, 2009

The role of liquid crystalline mesophases in polymer crystallization has seen increased attention following the observations of metastable liquid crystalline preordering in the crystallization of isotactic polypropylene and other flexible polymers.[1−7] In addition to these recent observations, in both nature and industry, liquid crystal mesophases are used to create polymeric materials with desirable properties such as spider silk[8] and Kevlar.[9] A better understanding of the theoretical fundamentals behind formation, kinetics, and morphological growth of polymer mesophases and their subsequent effect on crystallization would enable many new materials and processing techniques to be developed.

A recent study by Tokita et al.[10] on a polymer liquid crystal that exhibits a direct isotropic/smectic transition has experimentally determined the existence of metastable nematic orientational ordering preceding the formation of translational smectic ordering. This was accomplished through the study of a polymer liquid crystalline material BB-3(1-ME) that exhibits extremely slow liquid crystalline transition dynamics, also developed by Tokita et al.[11] The phase-ordering dynamics of this material occur at time scales accessible via conventional methods of polarized light scattering and synchrotron wide-angle X-ray diffraction analysis techniques.[10,11] Two key conclusions were determined from this work. First, at high quench rates/supercooling metastable nematic (orientational) ordering was observed preceding full smectic (orientational and translational) order. Second, the occurrence of nematic preordering (high supercooling) resulted in morphological changes of growing liquid crystalline domains compared to solely smectic growth (low supercooling). Specifically, samples cooled at rates high enough to exhibit nematic preordering formed well-oriented or "neat" tactoidal smectic domains while samples cooled at lower rates, where only smectic ordering was observed, formed radially oriented or textured spherulitic domains. It is noted that tactoids are ubiquitous transient nonspherical drops frequently observed in phase transformations involving mesophases.[12,13]

The objective of this Communication is to show that the essential features of the experimental observations of Tokita et al.[10] described above emerge from mesophase phase transformation phenomena as described by well-established phenomenological Landau−de Gennes type models.

The existence of metastable preordering in phase-ordering growth, where the order parameter is nonconserved (such as orientation), was first demonstrated theoretically by Bechhoefer et al.[14] and later for dual nonconserved order parameter systems.[15] In this past work, Landau−Ginzburg phase transition models composed of scalar order parameters were shown to exhibit a front-splitting instability under strong supercooling and also predicted this to occur when large differences in transition time scales exist.

The scalar models used by Bechhoefer et al.[14,15] capture the basic preordering phenomena but are not suitable for comparison to experimental observations. This is especially true for liquid crystalline materials where phase ordering introduces additional physics due to inherent anisotropy (see Figure 1). Smectic liquid crystals include dual phase-ordering phenomena where orientational order is required for translational order to exist. Thus, with such a system three general effects influence the possible observation of metastable preordering: (1) the driving potential (as a function of temperature, concentration, and pressure), (2) energetic coupling between the two types of order, and (3) phase transition kinetics (difference in time scales governed by viscosity ratio).

In this Communication we demonstrate that the use of a high-order model and numerical simulation is able bridge the gap between the experimental observations of Tokita et al.[10] and the fundamental observations of Bechhoefer et al.[14−17] As will be shown, this approach both captures metastable nematic preordering in addition to actual multiscale dynamic texturing processes. A high-order Landau−de Gennes type phenomenological model[18,19] for the direct isotropic/smectic-A liquid crystalline transition is used with material parameters based on the 12CB (dodecylcyanobiphenyl) liquid crystal. This model does not take into account microstructure that is present in polymer liquid crystals but is an adequate first-approximation for the system studied by Tokita et al.[10] The variation of the time scales of nematic (orientational) and smectic-A (translational) ordering is easily achieved with this model, and ideal quenches are assumed. The effects of changing the energetic coupling between the orientational and translational ordering of the smectic-A mesophase, in addition to convection and heat of transition, are left to future work in that determination of a suitable set of phenomenological constants and model extensions are nontrivial tasks.[20]

Theoretical characterization of orientational and translational order is accomplished using order parameters that adequately capture the physics involved. Partial orientational order of the nematic phase is characterized using a symmetric traceless tensor:[18]

$$\mathbf{Q} = S\left(\mathbf{nn} - \frac{1}{3}\mathbf{I}\right) + \frac{1}{3}P(\mathbf{mm} - \mathbf{ll}) \tag{1}$$

where $\mathbf{n}$, $\mathbf{m}$, and $\mathbf{l}$ are the eigenvectors of $\mathbf{Q}$, which characterize the average molecular orientational axes, and S and P are scalars which characterize the extent to which the molecules conform to the average orientational axes.[21−23] Uniaxial order is characterized by S and $\mathbf{n}$, which correspond to the maximum eigenvalue (and its corresponding eigenvector) of $\boldsymbol{Q}$, $S = {}^3/_2\mu_n$. Biaxial order is characterized by P and $\mathbf{m}$, $\mathbf{l}$, which correspond to the lesser eigenvalues and eigenvectors, $P = {}^3/_2(\mu_m - \mu_l)$.

The one-dimensional translational order of the smectic-A mesophase in addition to the orientational order found in nematics is characterized through the use of primary (orientational) and secondary (translational) order parameters together.[24] A complex order parameter can be used to characterize translational order:[18]

$$\Psi = \psi e^{i\phi} = A + iB \tag{2}$$

*Corresponding author. E-mail: nasser.abukhdeir@mcgill.ca.

Published on Web 05/13/2009

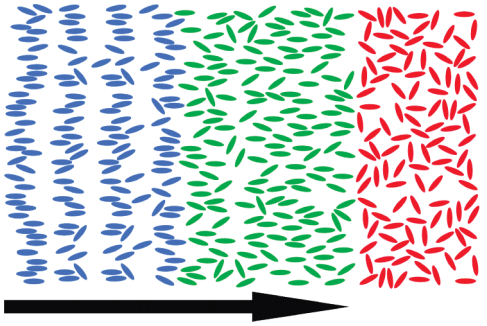

Figure 1. Schematic of a growing liquid crystalline front summarizing the phenomena of interest: nematic (orientational) and smectic-A (lamellar) liquid crystalline ordering and interfacial splitting. The orientationally/translationally ordered smectic-A mesophase is on the left (blue), orientationally ordered nematic mesophase is in the center (green), and the isotropic liquid (no orientational or translational order) is on the right (red).

where ϕ is the phase, ψ is the scalar amplitude of the density modulation, and A/B is the real/imaginary component of the complex order parameter. The density wave vector, which describes the average orientation of the smectic-A density modulation, is defined as $\mathbf{a} = \nabla\phi/|\nabla\phi|$. The smectic scalar order parameter ψ characterizes the magnitude of the density modulation and is used in a dimensionless form in this work. In the smectic-A mesophase the preferred orientation of the wave vector is parallel to the average molecular orientational axis, **n**.

A Landau−de Gennes type model for the first order isotropic/smectic-A phase transition is used that was initially presented by Mukherjee, Pleiner, and Brand[18,19] and later extended by adding nematic elastic terms:[25−27]

$$\begin{aligned} f - f_0 = {} & \frac{1}{2}a(\mathbf{Q}:\mathbf{Q}) - \frac{1}{3}b(\mathbf{Q}\cdot\mathbf{Q}):\mathbf{Q} + \frac{1}{4}c(\mathbf{Q}:\mathbf{Q})^2 + \\ & \frac{1}{2}\alpha|\Psi|^2 + \frac{1}{4}\beta|\Psi|^4 - \frac{1}{2}\delta|\Psi|^2(\mathbf{Q}:\mathbf{Q}) - \\ & \frac{1}{2}e\mathbf{Q}:(\nabla\Psi)(\nabla\Psi^*) + \frac{1}{2}l_1(\nabla\mathbf{Q})^2 + \\ & \frac{1}{2}l_2(\nabla\cdot\mathbf{Q})^2 + \frac{1}{2}l_3\mathbf{Q}:(\nabla\mathbf{Q}:\nabla\mathbf{Q}) + \\ & \frac{1}{2}b_1|\nabla\Psi|^2 + \frac{1}{4}b_2|\nabla^2\Psi|^2 \end{aligned} \quad (3)$$

$$a = a_0(T - T_{\mathrm{NI}})$$

$$\alpha = \alpha_0(T - T_{\mathrm{AI}})$$

where f is the free energy density, f_0 is the free energy density of the isotropic phase, terms 1−5 are the bulk contributions to the free energy, and terms 6−7 are couplings of nematic and smectic order; both the bulk order and coupling of the nematic director and smectic density-wave vector, respectively. Terms 8−10/11−12 are the nematic/smectic elastic contributions to the free energy. T is temperature, $T_{\mathrm{NI}}/T_{\mathrm{AI}}$ are the hypothetical second-order transition temperatures for isotropic/nematic and isotropic/smectic-A mesophase transitions (refer to ref 28 for more details), and the remaining constants are phenomenological parameters.

The Landau−Ginzburg time-dependent formulation[29] is used to capture the dynamics of the phase transition. The general form of the time-dependent formulation is as follows:[29]

$$\begin{pmatrix} \frac{\partial \mathbf{Q}}{\partial t} \\ \frac{\partial A}{\partial t} \\ \frac{\partial B}{\partial t} \end{pmatrix} = \begin{pmatrix} \frac{1}{\mu_{\mathrm{n}}} & 0 & 0 \\ 0 & \frac{1}{\mu_{\mathrm{S}}} & 0 \\ 0 & 0 & \frac{1}{\mu_{\mathrm{S}}} \end{pmatrix} \begin{pmatrix} -\frac{\delta F}{\delta \mathbf{Q}} \\ -\frac{\delta F}{\delta A} \\ -\frac{\delta F}{\delta B} \end{pmatrix} \quad (4)$$

$$F = \int_V f \, \mathrm{d}V \quad (5)$$

where $\mu_{\mathrm{r}}/\mu_{\mathrm{s}}$ is the rotational/smectic viscosity and V the volume. A higher order functional derivative must be used due to the second-derivative term in the free energy equation (3):

$$\frac{\delta F}{\delta \theta} = \frac{\partial f}{\partial \theta} - \frac{\partial}{\partial x_i}\left(\frac{\partial f}{\partial \frac{\partial \theta}{\partial x_i}}\right) + \frac{\partial}{\partial x_i}\frac{\partial}{\partial x_j}\left(\frac{\partial f}{\partial \frac{\partial^2 \theta}{\partial x_i \, \partial x_j}}\right) \quad (6)$$

where θ corresponds to the order parameter.

As shown below, in this Communication we capture the essential experimental results[10] by varying the quench depth and the translational/rotational viscosity ratio. This choice follows from the fact that the phase transformation velocity is given by ratio of the temperature-controlled free energy driving force and the viscosity associated with mesophase ordering.[30] This is first studied by treating the kinetic phase transformation process as a one-dimensional propagation transition front(s), where the unstable isotropic phase is replaced by the stable smectic-A phase. Multiple one-dimensional simulations were conducted for different viscosity ratio/quench depth values and the smectic-A/metastable nematic front behavior characterized. These results were then used to determine a dynamic phase diagram in order to guide higher dimensional simulations. Following this, a pair of two-dimensional simulations were performed in regimes where metastable nematic ordering is (1) not present and (2) present, guided by the previously determined dynamic phase diagram. All computational results were achieved by the simulation of eq 4, using the same computational methods defined in ref 20. These two stages of the presented work correspond directly to the two key conclusions of the experimental work of Tokita et al.[10]

Previous work for phenomenological parameter determination (parameters in eq 3) and phase diagram computation has been completed for this system[20] which shows that a definite free energy minimum exists corresponding to smectic-A order. In addition, a degenerate nematic-order state exists below the theoretical second-order transition temperature T_{AI} for this system. Figure 2a shows the free energy density (3) versus quench depth ($\Delta T = T_{\mathrm{AI}} - T$) for both neat smectic-A and degenerate nematic order as predicted by the model. As mentioned previously, one-dimensional homeotropic front growth was studied by varying the difference in time scales for the formation of nematic and smectic-A order, $\mu^* = \mu_{\mathrm{S}}/\mu_{\mathrm{N}}$, and the magnitude of the driving variable, temperature quench depth ΔT. Figure 2b shows the computed dynamic growth phase diagram where three distinct regimes can be identified:

1. Fully coupled (FC, lower left region): in this regime nematic and smectic-A interfaces cannot be distinguished and correspond to the direct transition from an isotropic to smectic-A phase. In other words, the nematic preordering layer is not observed.

2. Static decoupled (SDC, middle region): in this regime metastable nematic preordering (see Figure 2a) is observed to proceed from the initial smectic-A front but maintains a constant

distance/halo and does not fully decouple. In this case, a constant thickness nematic preordering layer separates the unstable receding isotropic phase from the stable advancing smectic-A phase.

3. Fully decoupled (FDC, upper right region): in this regime metastable nematic preordering (see Figure 2a) is observed to proceed from the initial smectic-A front at a velocity greater than the preceding smectic-A front velocity. In this case, the preordering nematic layer replaces the isotropic phase and becomes the matrix in which the smectic-A phase grows. Note that biaxiality (see eq 1) can be neglected in this specific case of one-dimensional homeotropic front growth.

Next we identify the main mechanisms behind the results of Figure 2a. The effect of the quench depth ΔT on the kinetics of the phase-ordering transition is revealed by the work of Bechhoefer et al.[14,15] Whereas previous work on a dual nonconserved order parameter system focused on quench depth as the driving variable to induce the splitting instability,[15] the effect of differences in dynamic time scales of orientational and positional ordering can induce the same phenomenon. In the case of low molecular mass liquid crystals, as this model is most applicable, experimental observations point toward the FC regime. In the case of liquid crystalline polymers, where the time scale for local diffusion increases substantially compared to rotation (rigid/semirigid and side-chain liquid crystalline polymers), the contribution of the difference in time scales is predicted to exhibit this behavior at much lower quench depths, observed experimentally[10] and in agreement with the presented results (Figure 2b).

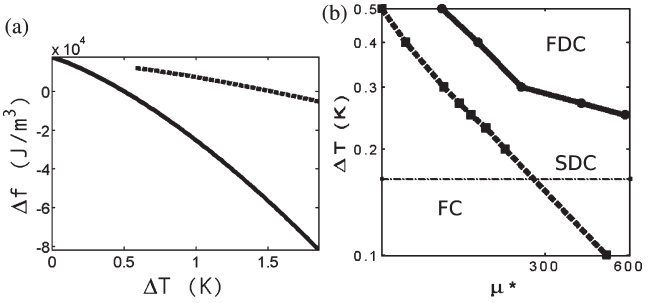

Figure 2. (a) Plot of free energy density versus quench depth $\Delta = T_{AI} - T$ for neat smectic-A order (solid line) and degenerate nematic order (dotted line). (b) Log−log plot of quench depth versus viscosity ratio $\mu^* = \mu_s/\mu_n$ (ratio of time scale of orientational and translational order) of the numerically determined SDC (squares/dotted line), FDC (circles/solid line) boundaries, and temperature at which the degenerate nematic phase becomes unstable (dot-dashed line); see text. The material parameters and phenomenological coefficients, based upon 12CB,[20] are $T_{NI} = 322.85$ K, $T_{AI} = 330.5$ K, $a_0 = 2 \times 10^5$ J/(m^3 K), $b = 2.823 \times 10^7$ J/m^3, $c = 1.972 \times 10^7$ J/m^3, $\alpha_0 = 1.903 \times 10^6$ J/(m^3 K), $\beta = 3.956 \times 10^8$ J/m^3, $\delta = 9.792 \times 10^6$ J/m^3, $e = 1.938 \times 10^{-11}$ pN, $l_1 = 1 \times 10^{-12}$ pN, $l_2 = 1.033 \times 10^{-12}$ pN, $b_1 = 1 \times 10^{-12}$ pN, $b_2 = 3.334 \times 10^{-30}$ J m, and $\mu_n = 8.4 \times 10^{-2}$ (N s)/m^2.

In order to examine the second experimental observation, that the presence of metastable nematic preordering induces persistent morphological changes of the liquid crystalline domain, simulation of the growth of an initially homogeneously oriented smectic-A spherulite was performed in two dimensions. This simulation was formed in the FDC growth regime (metastable nematic preordering) and compared to past work[31] on the same system in the FC growth regime (no preordering). Quasi-bulk conditions were imposed using full periodicity which results in an effective ensemble of well-oriented spherulites growing in an isotropic matrix. Figure 3a,b shows the spherulite morphologies at the maximum radius achievable with the current computational limitations (for the FDC simulation). The morphological growth process of the FC regime case is complex (refer to ref 31) but can be summarized as involving the competition between interfacial anchoring at the isotropic/smectic-A interface and bulk texturing. The resulting spherulite texture assumes a quasi-bipolar texture and exhibits an undulation instability in the bulk.[31] The effect of the fully formed metastable nematic matrix phase (Figure 3b) has a stabilizing field effect and exhibits tactoidal growth of a neat texture. The aspect ratio versus long axis (vertical in both cases) are shown in Figure 3c. The effects of nematic preordering are shown in the current simulation to have a strong morphological effect on the smectic-A spherulite, minimizing the previously observed interfacial anchoring effects and undulation instability. The well-oriented nematic matrix phase acts in the same way as a bulk electric/magnetic field,[32] which promotes tactoidal growth of a well-oriented smectic-A domain, consistent with the observations of Tokita et al.[10]

The aspect ratio trend for the FC regime simulation (Figure 3c) shows a decay, after an initial shape dynamic period, of the aspect ratio as the spherulite size increases. This decay is explained based upon a scaling theory derived from the studying shape and director-field transformation of nematic tactoids.[13,33] A scaling estimate for the aspect ratio of the spherulite was determined to obey the following relationship to minimize total free energy:[33]

$$\frac{R}{r} \approx K^{3/5}\tau^{-3/5}V^{-1/5} \tag{7}$$

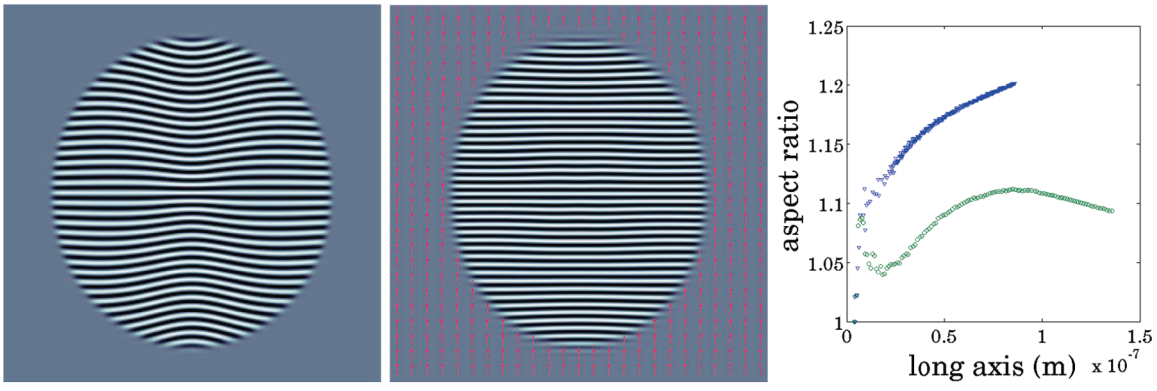

Figure 3. Two-dimensional simulation results of the growth of an initially homogeneously oriented smectic-A spherulite without (a) ($\mu^* = 25$) and with metastable nematic preorder (b) ($\mu^* = 25$) where the surface corresponds to Re(Ψ) (the smectic-A layers) and arrows denote the presence of nematic order and the director orientation (should be considered headless). (c) Plot of the aspect ratio versus long axis (vertical) of the simulations from (a) (circles) and with preordering (triangles). Other simulation parameters were used from Figure 2.

where R is the major axis and r is the minor axis, K is the characteristic Frank elastic constant, τ is interfacial tension, and V is the volume of the spherulite. Equation 7 predicts that the spherulite aspect ratio decreases with volume converging to 1, in agreement with Figure 3c.

For the FDC case, the stabilizing nematic preordering results in a spherulite with a neat texture and thus should obey the Wulf construction[34] which determines surface shape by minimizing the sum of total interfacial energy and an ideal undistorted bulk contribution:[34]

$$F = \int_A \gamma(\mathbf{r})\, \mathrm{d}A + \alpha V \tag{8}$$

where F is the total free energy of the spherulite, γ is the interfacial tension (a function of position $\mathbf{r}$), and α is the free energy density of the spherulite bulk. For the phenomenological parameters used in these simulations, planar anchoring (director parallel to the interface) is energetically preferred over homeotropic (director perpendicular to the interface). Figure 3b,c shows that this approximation correctly predicts tactoidal growth, maximizing the planar-anchored interfacial area.

The simulated system is one example of the possible effects of nematic preordering on the formation of a stable smectic-A domain. Past work[35,36] on the growth of initially homogeneously oriented nematic spherulites implies another possible scenario. In that work, deep quenches were found to result in the shedding of four $+^1/_2$ disclination defects in the nematic case. This is not morphologically what is proposed for the smectic-A case.[31] Thus, nematic preordering could result in a different smectic-A domain morphology due to difference in defect shedding characteristics of the preceding nematic front, which would serve as a template. These issues will be investigated in future work. Additionally, other phase transformations, such as metastable liquid−liquid demixing, have also been studied in this context.[37]

In conclusion, it has been shown that through simulation of a high-order Landau−de Gennes type model of the isotropic/smectic-A liquid crystalline transition experimental observations of nematic preordering of smectic liquid crystalline transitions[10] can be studied. Leveraging this type of high-dimensional model has been shown to close the gap between experimental observations of this phenomena[10] and generalized theoretical studies.[14−17] Phase transition kinetics results presented show that nematic preordering results from both thermodynamic potential and dynamic differences in phase-ordering time scales (Figure 2b), as was observed experimentally.[10] Two-dimensional simulation results presented explain the experimentally observed effect of nematic preordering on growth morphologies of smectic domains, where preordering of nematic domain stabilizes a neat texture in the growing smectic-A nucleus, promoting tactoidal growth. This work sets the basis for further simulation study in two/three dimensions and extension of the existing model[18,19] to account for the microstructure present in polymer liquid crystals. These results, in addition to those of Tokita et al.,[10] determine a possible mechanism for influencing the material properties of smectic polymer liquid crystals through the induction of metastable nematic preordering.

Acknowledgment. This work was supported by a grant from the Natural Science and Engineering Research Council of Canada.

Note Added after ASAP Publication. This Communication was published ASAP on May 13, 2009. Several changes have been made to equation 3 and throughout the text. The correct version was published on May 15, 2009.

References and Notes

(1) Imai, M.; Kaji, K.; Kanaya, T. *Phys. Rev. Lett.* **1993**, *71*, 4162–4165.
(2) Imai, M.; Kaji, K.; Kanaya, T. *Macromolecules* **1994**, *27*, 7103–7108.
(3) Matsuba, G.; Kaji, K.; Nishida, K.; Kanaya, T.; Imai, M. *Polym. J. (Tokyo)* **1999**, *31*, 722–727.
(4) Asano, T.; Balta-Calleja, F. J.; Flores, A.; Tanigaki, M.; Mina, M. F.; Sawatari, C.; Itagaki, H.; Takahashi, H.; Hatta, I. **1999**, *40*, 6475−6484.
(5) Ran, S.; Wang, Z.; Burger, C.; Chu, B.; Hsiao, B. *Macromolecules* **2002**, *35*, 10102–10107.
(6) Li, L.; de Jeu, W. H. *Phys. Rev. Lett.* **2004**, *92*, 075506/1–075506/3.
(7) Soccio, M.; Nogales, A.; Lotti, N.; Munari, A.; Ezquerra, T. A. *Phys. Rev. Lett.* **2007**, *98*, 037801.
(8) Vollrath, F.; Knight, D. *Nature (London)* **2001**, *410*, 541–548.
(9) Dobb, M.; Johnson, D.; Saville, B. *J. Polym. Sci., Polym. Phys. Ed.* **1977**, 15, year.
(10) Tokita, M.; Kim, K.-W.; Kang, S.; Watanabe, J. *Macromolecules* **2006**, *39*, 2021–2023.
(11) Tokita, M.; Funaoka, S.-i.; Watanabe, J. *Macromolecules* **2004**, *37*, 9916–9921.
(12) Dierking, I.; Russell, C. *Physica B* **2003**, *325*, 281–286.
(13) Prinsen, P.; Schoot, P. *Eur. Phys. J. E* **2004**, *13*, 35–41.
(14) Bechhoefer, J.; Lowen, H.; Tuckerman, L. S. *Phys. Rev. Lett.* **1991**, *67*, 1266–1269.
(15) Tuckerman, L. S.; Bechhoefer, J. *Phys. Rev. A* **1992**, *46*, 3178–3192.
(16) Evans, R.; Poon, W.; Cates, M. *Europhys. Lett.* **1997**, *38*, 595–600.
(17) Evans, R. M. L.; Cates, M. E. *Phys. Rev. E* **1997**, *56*, 5738–5747.
(18) de Gennes, P.; Prost, J. *The Physics of Liquid Crystals*, 2nd ed.; Oxford University Press: New York, **1995**.
(19) Mukherjee, P. K.; Pleiner, H.; Brand, H. R. *Eur. Phys. J. E* **2001**, *4*, 293–297.
(20) Abukhdeir, N.; Rey, A. Arxiv preprint arXiv **2008**, arXiv:0807.4525, year. Accepted for publication in *Commun. Comput. Phys.* 12MAR2009.
(21) Rey, A.; Denn, M. *Annu. Rev. Fluid Mech.* **2002**, *34*, 233.
(22) Yan, J.; Rey, A. D. *Phys. Rev. E* **2002**, *65*, 031713.
(23) Rey, A. D. *Soft Matter* **2007**, *3*, 1349–1368.
(24) Toledano, J.-C.; Toledano, P. *The Landau Theory of Phase Transitions: Application to Structural, Incommensurate, Magnetic, and Liquid Crystal Systems*; World Scientific Lecture Notes in Physics; World Scientific Publishing Co.: Singapore, **1987**.
(25) Brand, H. R.; Mukherjee, P. K.; Pleiner, H. *Phys. Rev. E* **2001**, *63*, 061708/1–061708/6.
(26) Mukherjee, P. K.; Pleiner, H.; Brand, H. R. *J. Chem. Phys.* **2002**, *117*, 7788–7792.
(27) Biscari, P.; Calderer, M.; Terentjev, E. *Phys. Rev. E* **2007**, *75*, 051707.
(28) Coles, H. J.; Strazielle, C. *Mol. Cryst. Liq. Cryst.* **1979**, *55*, 237–50.
(29) Barbero, G.; Evangelista, L. R. *An Elementary Course on the Continuum Theory for Nematic Liquid Crystals*; Series on Liquid Crystals; World Scientific Publishing Co.: Singapore, **2000**; Vol. *3*.
(30) Wincure, B.; Rey, A. *J. Chem. Phys.* **2006**, *124*, 244902.
(31) Abukhdeir, N.; Rey, A. Arxiv preprint **2009**, arXiv:0902.1544, year. Accepted for publication in *Liq. Cryst.* 09MAR2009.
(32) Das, S.; Rey, A. *Macromol. Theory Simul.* **2006**, *15*, 469.
(33) Prinsen, P.; van der Schoot, P. *Phys. Rev. E* **2003**, *68*, 021701.
(34) Virga, E. *Variational Theories for Liquid Crystals*; CRC Press: Boca Raton, FL, **1994**.
(35) Wincure, B.; Rey, A. *Continuum Mech. Thermodyn.* **2007**, *19*, 37–58.
(36) Wincure, B.; Rey, A. *Nano Lett.* **2007**, *7*, 1474–1479.
(37) Hu, W.; Frenkel, D. *Macromolecules* **2004**, *37*, 4336–4338.